Simple Approach to Stabilized Micelles Employing Miktoarm Terpolymers and Stereocomplexes with Application in Paclitaxel Delivery

Fredrik Nederberg,[†,‡] Eric Appel,[†] Jeremy P. K. Tan,[§] Sung Ho Kim,[†] Kazuki Fukushima,[†] Joseph Sly,[†] Robert D. Miller,[†] Robert M. Waymouth,[‡] Yi Yan Yang,*[,§] and James L. Hedrick*[,†]

IBM Almaden Research Center, 650 Harry Road, San Jose, California 95120, Department of Chemistry, Stanford University, Stanford, California 94305, and Institute of Bioengineering and Nanotechnology (IBN), 31 Biopolis Way, The Nanos, #04-10, Singapore 138669

Received January 15, 2009; Revised Manuscript Received March 11, 2009

A simple and versatile approach to miktoarm co- and terpolymers from carbonate functional oligomers is described. The key building block employed is a carboxylic acid functional cyclic carbonate, derived from 2,2-bis(methylol)propionic acid, that was readily coupled to a hydroxyl functional monomethylether poly(ethylene glycol) oligomer. Ring-opening of the cyclic carbonate using functional amines generates a carbamate linkage bearing a functional group capable of initiating either controlled radical or ring-opening polymerization, together with a primary hydroxyl group for ring-opening polymerization. Two tandem polymerization steps were possible which add the second two arms, thus generating the targeted ABC miktoarm terpolymer. The resulting amphiphilic miktoarm terpolymers containing poly(D- and L-lactide) formed polylactide stereocomplexes in the bulk. In aqueous solution, the stereocomplex mixture of Y-shaped miktoarm copolymers, poly(ethylene glycol)-poly(D-lactide)-poly(D-lactide) and poly(ethylene glycol)-poly(L-lactide)-poly(L-lactide), or the stereoblock miktoarm poly(ethylene glycol)-poly(D-lactide)-poly(L-lactide) form stabilized micelles with a significantly lower critical micelle concentration than those derived from conventional stereo regular linear or Y-shaped amphiphiles. This simple and versatile approach provides a useful synthetic route to complex macromolecular architectures that can assemble into stable micelles. These micelles provide high capacity for loading of the anticancer drug paclitaxel and possess narrow size distribution as well as unique structure, leading to sustained and near zero-ordered release of drug without significant initial burst.

Introduction

Progress in controlled or living polymerization techniques combined with new synthetic methodologies and efficient organic reactions have had an enormous impact on the ease and level of control on polymer design for functional materials and complex architectures.[1] These structures provided solutions to a number of technical challenges including template design,[2] drug delivery,[3] and self-assembly.[4] For example, molecularly defined and functional dendritic structures have been shown to be a promising new platform for the delivery of pharmaceuticals.[3] Star- and hyperbranched polymers are somewhat less defined materials but are synthetically more accessible than dendrimers, and they have found numerous applications including microelectronics.[5] Block copolymers may form different morphologies through self-assembly, and recent advances in directed self-assembly have demonstrated pattern transfer to underlying substrates.[6] Similarly, dendritic-linear[2c,7] and triblock copolymers[8] have also been found to exhibit distinct morphologies in both solution and bulk as a result of their unique architectures.

We have developed a range of organic catalysts for controlled or living ring-opening polymerization (ROP), including carbenes,[9] thiourea based catalysts,[10] and strong organic bases.[11,12] Narrowly dispersed polymers of predictable molecular weight and end-group fidelity can be readily generated by these methods. Moreover, these catalysts enable the generation of complex architectures including H-shaped polymers[13] as well as cyclic polymers.[14] A general platform for the preparation of functional materials from the organocatalytic ROP of protected cyclic carbonates has also been applied to the generation of network or thermosetting architectures from cyclic carbonate functional prepolymers.[15] Similarly, Frechet et al. demonstrated the functionalization of the hydroxyl end groups on a dendrimer periphery with a cyclic carbonate, followed by reaction with an amine to generate the carbamate and a primary alcohol on ring-opening.[16] Moreover, Endo demonstrated polyaddition between diamines and dicarbonates as a green route to polyurethanes.[17]

Paclitaxel, one of the best antineoplastic drugs, found from nature has excellent therapeutic effects against a wide spectrum of cancers including ovarian, breast, and colon cancer.[18] However, it has limited solubility in water (0.3 mg/L at 37 °C), making application of paclitaxel in cancer therapy difficult. Taxol is the only formulation available for clinical use, where paclitaxel is dissolved in a 50:50 mixture of Cremophore EL (polyethoxylated castor oil) and dehydrated alcohol. This is known to create serious side effects including hypersensitivity reactions, nephrotoxicity, cardiotoxicity, and neurotoxicity.[19] Thus, various polymer-based carriers like microspheres,[20] nanoparticles,[21] and micelles[22] have been explored with a

* To whom correspondence should be addressed. E-mail: hedrick@almaden.ibm.com (J.L.H.); yyyang@ibn.a-star.edu.sg (Y.Y.Y.).
† IBM Almaden Research Center.
‡ Stanford University.
§ Institute of Bioengineering and Nanotechnology (IBN).

10.1021/bm900056g CCC: $40.75
Published on Web 04/22/2009

Scheme 1. Conceptual Route to Miktoarm ABC Terpolymers Utilizing Nitroxide Mediated Polymerization (NMP) and Ring-Opening Polymerization (ROP)

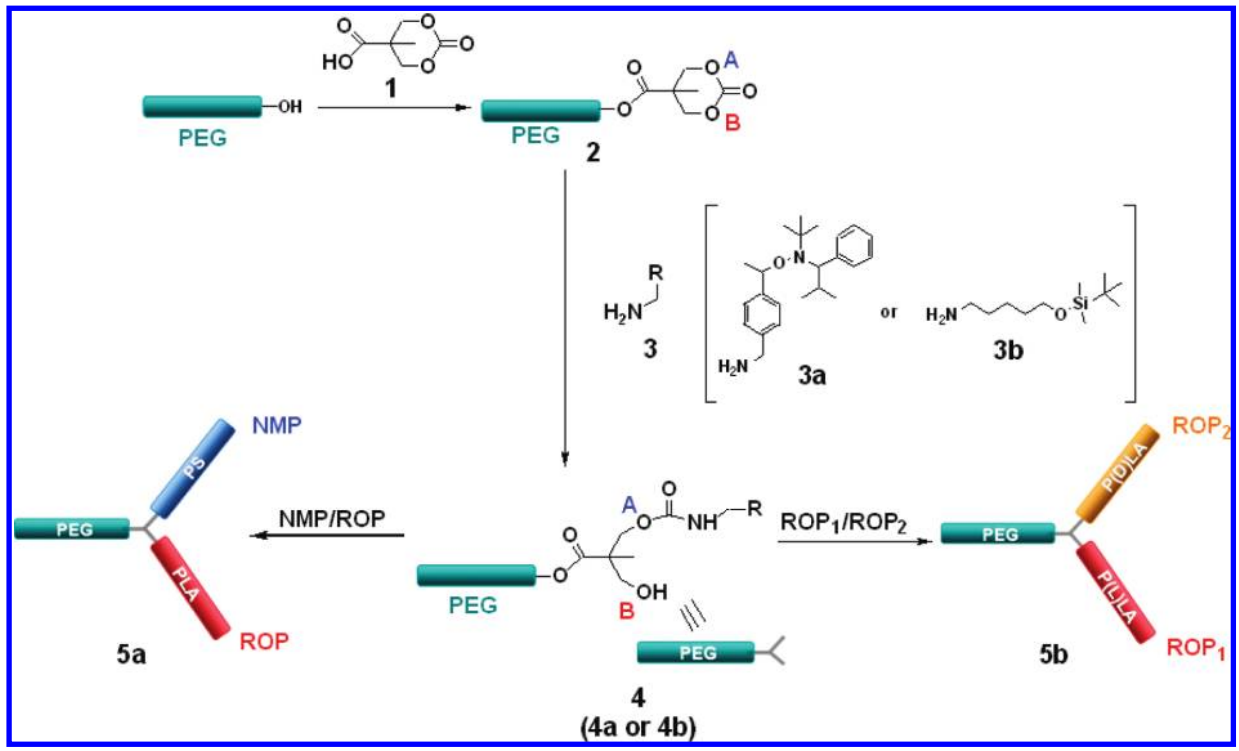

growing need to develop an alternative and efficient delivery system. Among them, biodegradable nanosized micelles are more advantageous than other carriers due to their ability of achieving passive targeting to leaky tumor tissues, and their well-defined core/shell structure having a hydrophilic shell for avoiding uptake of the reticuloendothelial system (RES), which prolongs blood circulation of the drug. However, one major problem associated with conventional polymeric micelles is inefficiency in paclitaxel loading because of its strong tendency of self-assembly into macrofibers,[23,24] and paclitaxel loading level was around 2−3% in weight.[25] Therefore, there is a need to design unique polymer architecture so that it can break down self-assembly of paclitaxel and promote the loading of paclitaxel into the cores of the micelles.

Here, we describe a simple and versatile approach to miktoarm[26] co- and terpolymers from carbonate functional oligomers, the general synthetic route given in Scheme 1. As the key building block, we focused on a carboxylic acid functional carbonate, **1**, derived from 2,2-bis(methylol)propionic acid (bis-MPA), a common building block for biodegradable dendrimers,[5a,b,16] that is readily coupled to a hydroxyl functional monomethyl ether poly(ethylene glycol) (PEG) oligomer and form cyclic carbonate functionalized PEG oligomer, **2**. The cyclic carbonate is ring-opened using functional amines, **3**, that generate one carbamate linkage bearing the functionality together with a primary hydroxyl group, **4**. Two subsequent polymerization steps were possible that add the second two arms, generating the targeted ABC miktoarm terpolymers, **5a** or **5b**, for specific applications (Scheme 1). For proof of concept, we demonstrate that the stereocomplexes formed from PEG-P(L)LA-P(D)LA or a mixture of PEG-P(D)LA-P(D)LA and PEG-P(L)LA-P(L)LA, which are synthesized using this approach, are able to load paclitaxel into nanosized micelles with high capacity and provide near zero-ordered release kinetics of paclitaxel without significant initial burst.

Experimental Section

Materials. Acid functional carbonate, **1**,[15a] monomethylether-PEG-carbonate, **2**,[15b] 2,2,5-trimethyl-3-(1′-*p*-aminomethylphenylethoxy)-4-phenyl-3-azahexane, **3a**,[27] and thiourea catalyst,[10b] were described elsewhere. Styrene (Aldrich) was filtered through activated aluminum oxide prior of use. L-Lactide, D-lactide, and *rac*-lactide (Bohringer-Ingelheim) were azeotropically dried from toluene and recrystallized prior of use. Monomethylether PEG (Fluka and Polymer source) was azeotropically dried from toluene prior of use. 5-Amino-1-pentanol, imidazole, *t*-butyl-chloro-dimethylsilane, acetic anhydride, and boron trifluoride diethyletherate were used as received. Dry CH_2Cl_2 was obtained by using a solvents drying system from Innovative.

Synthesis of Silyl-Protected 5-Amino-1-pentanol, 3b. 5-Amino-1-pentanol (10 g, 96.9 mmol, 1 equiv), imidazole (9.90 g, 145.4 mmol, 1.5 equiv), and 150 mL of methylene chloride were added to a flask and cooled to 0 °C. *tert*-Butyl(chloro)dimethlsilane (21.9 g, 145.4 mmol, 1.5 equiv) in 50 mL of methylene chloride was added dropwise. Once added the reaction mixture was warmed to room temperature and allowed to stir for 4 h. The mixture was then heated to 40 °C for an additional 2 h. Purification was performed by first washing with brine solution and then by column chromatography using pure ethyl acetate. ^{1}H NMR ($CDCl_3$, 400 MHz): δ 2.0−1.0 (m, 10H, -HN-(CH_2)$_5$-O-), 0.87 (s, 9H, *t*-bu), 0.03 (s, 6H, H_3C-Si-CH_3).

Procedure for Ring-Opening of Monomethylether-PEG-Carbonate with Functional Amine, 4. Monomethylether-PEG-carbonate (M_n 5000 g/mol, PDI 1.02, 5 g, 1 mmol, 1 equiv) was dissolved in dry methylene chloride (10 mL, 0.1 M). Functional amine (H_2N-R, 5 mmol, 5 equiv) was added, and the reaction mixture was left under stirring overnight (∼14 h) at room temperature. The crude polymer was purified by polymer precipitation into cold diethyl ether and dried under vacuum until a constant weight was reached. ^{1}H NMR ($CDCl_3$, 400 MHz): If amine alkoxyamine, **4a**: δ 7.50−7.00 (m, 9H, ArH), 4.90 (m, 1H), 4.40−3.80 (m, mixture), 3.85 (s, 4H, PEG), 3.38 (s, 3H, CH_3-O-), 1.6−0 (m, mixture alkoxyamine and CH_3). If silyl protected 5-amino-1-pentanol, **4b**: δ 4.23−3.70 (m, 7H, mixture), 3.62 (s, 284H, -O-CH_2-CH_2-O-), 3.55 (s, 3H, CH_3-O-), 2.0−1.0 (m, 10H, mixture), 0.87 (s, 9H, *t*-bu), 0.03 (s, 6H, H_3C-Si-CH_3).

Typical Procedure for Polymerization of Styrene Using NMP for the Addition of the Second Arm (Step 1 for 5a). PEG-nitroxide macroinitiator, **4a** (0.45 g, 90 μmol), and 0.7 g (6.75mmol for a DP of 75) of styrene were charged in a Schlenk-tube. Three pump−freeze−thaw cycles were performed to effectively degas the solution before the reaction vessel was heated to 125 °C and kept for a reaction time yielding ~85% monomer conversion (as judged from ^{1}H NMR analysis). Following the reaction, the crude product was cooled to room temperature after which THF was added (~10 mL) and the polymer was purified by precipitation in cold methanol. ^{1}H NMR ($CDCl_3$, 400 MHz): δ 7.50−6.30 (m, PS), 3.80−3.55 (s, PEG), 3.40 (s, 3H, CH_3O-), 2.40−1.20 (m, PS), 1.0−0.2 (mixture, alkoxyamine).

Typical Procedure for Polymerization of L-Lactide Using ROP for Addition of the Second Arm and Capping of the Hydroxyl End-Group with Acetic Anhydride (Step 1 for 5b). PEG-OH macroinitiator, **4b** (0.5 g, 0.1 mmol), thiourea catalyst (33 mg, 86.8 μmol), and (−)-sparteine (20.3 mg, 86.8 μmol) in 1.75 mL of methylene chloride was added to a solution of L-lactide (0.5 g, 3.47 mmol, $[LA]_0/[I]_0 = 35$) in 0.75 mL of methylene chloride. After 4 h of stirring at room temperature, acetic anhydride (51.1 mg, 0.5 mmol) was added, and the reaction mixture was stirred overnight at room temperature. The following morning the crude polymer was purified by precipitation into cold diethyl-ether. ^{1}H NMR ($CDCl_3$, 400 MHz): δ 5.15 (br, 63H, -COO-C*H*(CH_3)-O-), 4.23−3.70 (m, 7H, mixture), 3.62 (s, 284H, -O-CH_2-CH_2-O-), 3.55 (s, 3H, CH_3-O-), 1.55 (br, 189H, -COO-CH(CH_3)-O-), 2.0−1.0 (m, 10H, mixture), 0.87 (s, 9H, *t*-bu), 0.03 (s, 6H, H_3C-Si-CH_3).

Typical Procedure for Removal of the Silyl Group (Step 2 for 5b). PEG-P(L)LA macroinitiator (0.75 g, 75 μmol) was dissolved in 5 mL of methylene chloride and purged with N_2. Boron trifluoride diethyl etherate (0.5 mL, 4.05 mmol) was added under N_2 to the reaction flask and the mixture was sealed under N_2 and stirred at 40 °C overnight. Purification was performed by precipitation into cold diethyl ether the next morning. ^{1}H NMR ($CDCl_3$, 400 MHz): δ 5.15 (br, 63H, -COO-C*H*(CH_3)-O-), 4.23−3.70 (m, 7H, mixture), 3.62 (s, 284H, -O-CH_2-CH_2-O-), 3.55 (s, 3H, CH_3-O-), 1.55 (br, 189H, -COO-CH(CH_3)-O-), 2.0−1.0 (m, 10H, mixture).

Typical Procedure for Polymerization of D-Lactide Using ROP for Addition of the Third Arm (5a or 5b). PEG-PLLA-OH macroinitiator (0.5 g, 0.05 mmol), thiourea catalyst (16.5 mg, 43.4 μmol), and (−)-sparteine (10.2 mg, 43.4 μmol) in 0.75 mL of methylene chloride were added to a solution of D-lactide (0.25 g, 1.74 mmol, $[LA]_0/[I]_0 = 35$) in 0.375 mL of methylene chloride. The reaction mixture was stirred at room temperature for 4 h and precipitated into cold methanol to purify. ^{1}H NMR ($CDCl_3$, 400 MHz): δ 5.15 (br, 81H, -COO-C*H*(CH_3)-O-), 4.27 (m, 1H, -COO-C*H*(CH_3)-OH), 4.23−3.70 (m, 7H, mixture), 3.62 (s, 284H, -O-CH_2-CH_2-O-), 3.55 (s, 3H, CH_3-O-), 1.55 (br, 243H, -COO-CH(CH_3)-O-), 2.0−1.0 (m, 10H, mixture). The procedure is identical when polymerizing lactide from PEG-PS-OH macroinitiator.

Instrumentation. NMR spectra were recorded on a Bruker Avance 2000 (^{1}H NMR at 400 MHz, ^{13}C NMR at 100 MHz). Gel permeation chromatography (GPC) was performed in THF using a Waters chromatograph equipped with four 5 μm Waters columns (300 × 7.7 mm) connected in series with an increasing pore size (10, 100, 1000, 10^5, and 10^6 Å), a Waters 410 differential refractometer, and a 996 photodiode array detector and calibrated with polystyrene standards (750 to 2×10^6 g mol^{-1}).

Differential scanning calorimetry (DSC) was performed using a TA Differential Scanning Calorimeter 1000 that was calibrated using high purity indium at a heating rate of 10 °C/min. Melting points were determined from the second scan following slow cooling (to remove the influence of thermal history) at a heating rate of 10 °C/min.

Fluorescence Measurements. The critical micelle concentration (CMC) of the polymer in deionized (DI) water was determined by fluorescence spectroscopy using pyrene as the probe. The fluorescence spectra were recorded by a LS 50B luminescence spectrometer (PerkinElmer, United States) at 25 °C. Samples were equilibrated for 10 min before any measurements were made. Aliquots of pyrene in acetone solution (6.16×10^{-5} M, 10 μL) were added to containers, which were left in air to evaporate acetone. Polymeric solutions (1 mL) at varying concentrations were added into the pyrene containers and left to equilibrate for 24 h. The final pyrene concentration in each sample is 6.16×10^{-7} M. The emission spectra were scanned from 360 to 410 nm at an excitation wavelength of 339 nm, while the excitation spectra were scanned from 300 to 360 nm at an emission wavelength of 395 nm. Both the excitation and emission bandwidths were set at 2.5 nm. The intensity (peak height) ratio of I_{337}/I_{334} from the excitation spectra was analyzed as a function of polymer concentration (Figure S2). The CMC was taken from the intersection between the tangent to the curve at the inflection and tangent of the points at low concentration.

Laser Light Scattering Measurements. Dynamic light scattering (DLS) and static light scattering (SLS) experiments of the freshly prepared micelles were performed on a Brookhaven BI-200SM goniometer system (Brookhaven, United States) to determine the particle size (R_h) and weight average molecular weight (M_w), respectively. Briefly, polymer solution with a concentration of 0.5 mg/mL was prepared and filtered using 0.45 μm PVDF filter before measurement was conducted. After the measurement, non-negative least-squares (NNLS) were used to fit the distribution curve and the fitting obtained was found to be with a R^2 value of at least 0.98. A distribution curve is shown in Figure S3. The light source is a power adjustable vertically polarized 75 mW HeNe ion laser with a wavelength of 633 nm. For SLS, a Zimm plot (eq 1) was used to analyze the experimental data and the refractive index increment (dn/dc) was measured using a BI DNDC differential refractometer (Brookhaven, U.S.). A typical Zimm plot is shown in Figure S4. The aggregation number (N_w) was determined by the quotient of the micelle M_w and the unimer M_w and was measured at 25 °C.

$$\frac{Kc}{R_\theta} = \frac{1}{M_w}\left(1 + \frac{16\pi^2 n^2 R_g^2 \sin^2\left(\frac{\theta}{2}\right)}{3\lambda^2}\right) + 2A_2c \qquad (1)$$

where K ($= 4\pi^2 n^2 (\mathrm{d}n/\mathrm{d}c)^2 / N_A \lambda^4$) is an optical constant, R_θ ($= I_s r^2 / I_t \sin\theta$) is the Rayleigh ratio, c is the concentration of the polymer solution in gram per milliliter, n is the refractive index of the solvent, θ is the angle of measurement, λ is the wavelength of the laser in vacuum, and N_A is the Avogadro's constant. A plot of (Kc/R_θ) against ($\sin^2(\theta/2) + kc$) (where k is a plotting constant) and extrapolating the data to zero angles and concentrations, radius of gyration (R_g) and second viral coefficient (A_2) can be obtained from the slopes, respectively. A simultaneous extrapolation to zero angle and concentration yields an intercept that is the inverse of M_w.

Paclitaxel-Loaded Micelles. Encapsulation of paclitaxel into Y-shaped PEG-PLA block copolymer micelles was performed through a sonication/membrane dialysis method. Briefly, 5 mg of block copolymer (i.e., Y-shaped PEG-P(D)LA-P(D)LA (5k-2k-2k) and PEG-P(L)LA-P(D)LA (5k-2k-2k) or a mixture of PEG-P(L)LA-P(L)LA (5k-2k-2k) and PEG-P(D)LA-P(D)LA (5k-2k-2k) in 1:1 weight ratio) and paclitaxel (1 mg) were dissolved in 1 mL of acetone. The drug and polymer solution was added dropwise to DI water (10 mL) when being sonicated at 130 W using a probe-based sonicator (Vibra Cell VCX 130), and the sonication lasted for 10 min. The solution was then dialyzed against 1000 mL of DI water for 48 h using a dialysis bag with molecular weight cutoff of 1000 Da (Spectra/Por 7, Spectrum Laboratories Inc.). The water was changed every 2 h for the first 6 h and once again the next day. After dialysis, the samples were harvested by lyophilization.

Determination of Paclitaxel Loading. The final paclitaxel content in the micelles was determined by high performance liquid chromatography (HPLC). Briefly, freeze-dried paclitaxel-loaded micelles (1 mg) were first dissolved in 1 mL of chloroform, and 5 mL of diethyl ether was then added to precipitate the polymer. The resultant mixture was centrifuged at 4000 rpm for 10 min, and the supernatant was removed and air-dried. Mixed solvent of 20 mM ammonium acetate,

Scheme 2. Synthetic Route to PEG-PS-PLA Miktoarm Architectures Employing a Tandem NMP/ROP Approach[a]

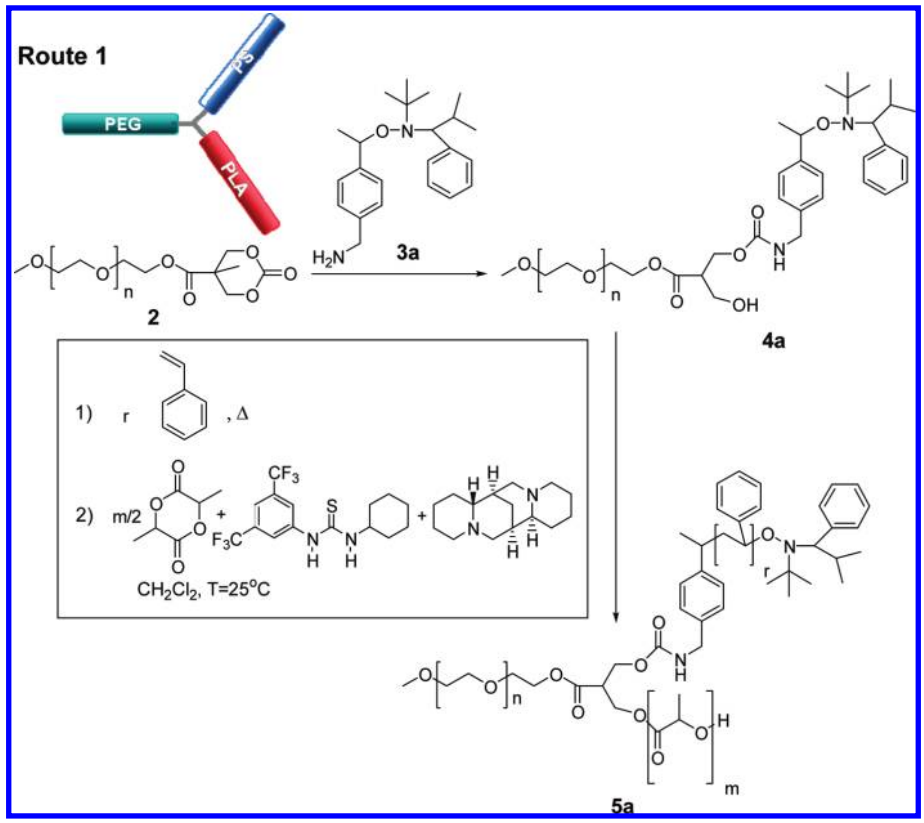

[a] Inset shows the steps to add the two additional arms.

methanol, and acteonitrile (35:20:45 in volume; HPLC mobile phase, 2 mL) was added to dissolve the sample, which was filtered with a 0.45 μm syringe filter prior to HPLC analysis. The HPLC system consisted of a Waters 2690 separation module fitted with a Waters 996 Photodiode Array Detector and Waters XBridge C_8 46 × 150 mm column. The elution rate was set at 1 mL/min and the paclitaxel detection wavelength was set at 228 nm. The column and sample temperature was maintained at 28 and 15 °C, respectively. A calibration line was constructed to determine paclitaxel concentration in the range of 0.1 to 50 mg/L, and the r^2 value of peak area intensity plotted linearly against paclitaxel concentration was at least 0.999. The paclitaxel recovery rate after polymer precipitation in diethyl ether was determined to be 90%. The paclitaxel loading level was calculated based on the following formula:

$$\text{actual loading level(wt\%)} = \frac{\text{mass of paclitaxel extracted from micelles}}{\text{mass of drug-loaded micelles}} \times 100\% \quad (2)$$

In Vitro Paclitaxel Release Experiment. The freeze-dried paclitaxel-loaded sample was dissolved in PBS buffer (pH 7.4) at a concentration of 1 mg/mL. The solution was transferred into a dialysis bag with a molecular weight cutoff of 1000 Da (Spectra/Por 7, Spectrum Laboratories Inc.). The bag was then immersed into a container with 50 mL of PBS, with shaking at 100 rev/min at 37 °C. At specific time intervals, the entire medium was removed and replaced with fresh buffer. Paclitaxel was extracted from the release medium by adding 5 mL of DCM, and the mixture was vigorously vortexed for 3 min. Upon phase separation, the DCM phase was extracted and left to evaporate overnight. The solid samples were dissolved in 2 mL of the mobile phase and analyzed by HPLC. The experiment was repeated in triplicate. The extraction efficiency of paclitaxel from the release medium was determined to be 90%.

Transmission Electron Microscopy (TEM). The morphologies of the micelles were observed under a FEI Tecnai G^2 F20 electron microscope using an acceleration voltage of 200 keV. To prepare the TEM samples, several drops of the micelles solution containing 0.2% (w/v) of phosphotungstic acid, which were incubated for 30 min, were placed on a Formvar/carbon-coated 200 mesh copper grid and left to dry under room temperature.

Results and Discussion

In Schemes 2 and 3 are depicted two different synthetic routes to mikto-architectures demonstrating the versatility of this approach. In the first example (Scheme 2), an amine functionalized alkoxy amine was utilized to open the terminal carbonate to generate a carbamate linkage bearing two orthogonal initiating functionalities that enabled a sequential controlled radical polymerization (CRP) (that is nitroxide-mediated polymerization (NMP)) and an alcohol-initiated ring-opening polymerization (ROP). In a second example (Scheme 3), aminopentanol or a protected aminopentanol open the carbonate generating two hydroxyl initiators for concurrent or sequential ROP of lactide to generate miktoarm copolymers with different tacticities and absolute configurations on the two arms. We, in addition, demonstrate that amphiphilic miktoarm terpolymers capable of stereocomplexation[29] between two enantiomeric poly(lactide)s generate stable micelles with low critical micelle concentration (CMC). Stereocomplex formation was achieved by incorporating the L- and D-enantiomers of lactide, respectively, when constructing the subsequent two arms using ROP.

To generate the requisite macroinitiators, carbonate functionalized monomethyl ether PEG was prepared by acylation of the hydroxyl functional PEG with an acid functional cyclic carbonate using DCC according to a literature procedure.[15b] Ring-opening of this carbonate with the amine functional alkoxy amine was carried out in methylene chloride (0.1 M), generating a carbamate linked bifunctional macroinitiator which was

Scheme 3. Synthetic Route to PEG-P(L)LA-P(D)LA Miktoarm Architectures Employing Two ROP Steps[a]

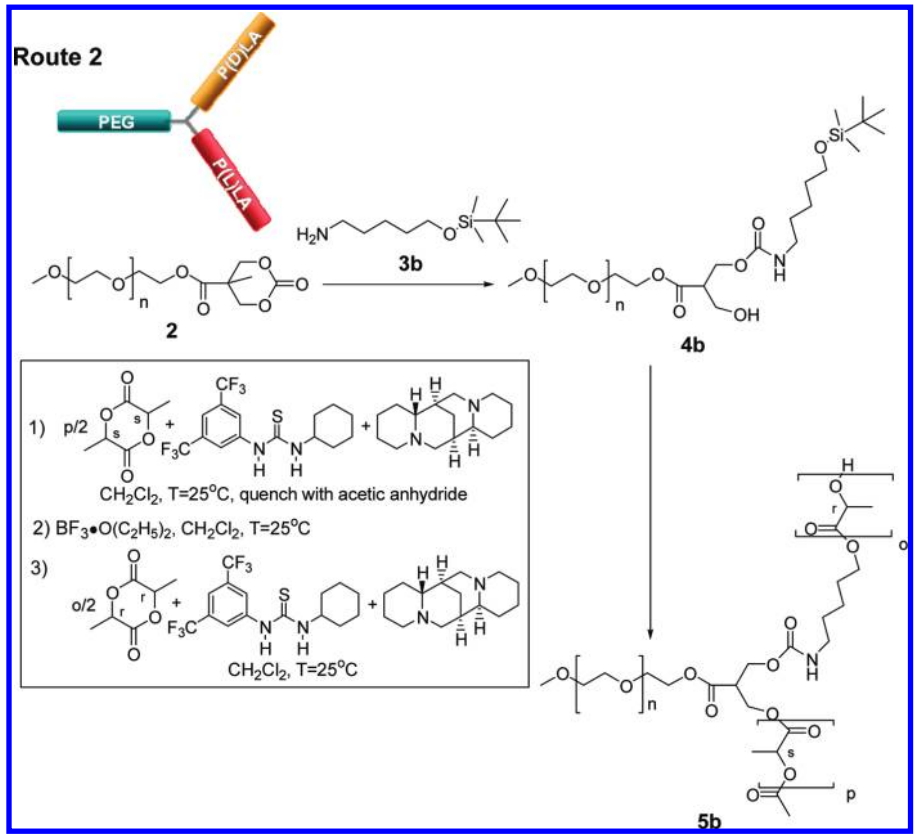

[a] Inset shows the necessary steps to add the two additional arms.

Table 1. Characteristics of PEG-PS-P(L)LA, and PEG-PLA-PLA Miktoarm Terpolymers

structure	M_n[a] (g/mol)	PDI = M_w/M_n[a]
PEG	7300	1.02
PEG-PS	9200	1.16
PEG-PS-P(L)LA	15200	1.15
PEG-P(L)LA-P(L)LA	16500	1.09
PEG-P(D)LA-P(D)LA	15900	1.09
PEG-P(*rac*)LA-P(*rac*)LA	15000	1.09
PEG-P(L)LA	9200[b]	1.07
PEG-P(L)LA-P(D)LA	14500[b]	1.07

[a] From GPC measurements (THF) calibrated with polystyrene standards and refractive index detector. [b] From ^{1}H NMR end-group analysis.

purified by simple precipitation in cold diethyl ether.[16] The nitroxide-mediated polymerization (NMP) of styrene with a targeted degree of polymerization (DP) of 50 was accomplished in bulk conditions at 120 °C, and the resulting diblock copolymer was isolated by precipitation in methanol (~85% conversion, Table 1). Subsequent ROP of L-lactide initiated from the pendent hydroxyl group (at a $[M]_0/[I]_0 = 35$) was performed at room temperature in methylene chloride using a thiourea/sparteine catalyst/cocatalyst system to generate the ABC miktoarm terpolymer (PEG-PS-P(L)LA, Table 1). Gel permeation chromatography (GPC) and ^{1}H NMR (Figure 1) spectroscopy were used to follow each of these transformations. The GPCs clearly show clean and quantitative transformations with no evidence of homopolymer contamination as demonstrated by the narrow, monomodal molecular weight distributions (Table 1).[28] Moreover, the molecular weight increased from ~7300 g/mol to 15000 g/mol, consistent with the targeted DP for each of the blocks (Table 1). The ^{1}H NMR spectra of the terpolymer (Figure 1) clearly shows the expected peaks from each of the blocks together with their respective end-group (i.e., PEG methoxy methyl singlet at 3.40 ppm, PS alkoxyamine at 1.0−0.5 ppm (*t*-butyl group), and PLA end-group quartet at ~4.35 ppm).

To further demonstrate the efficacy of the ring-opening of carbonate functional PEG oligomers to generate interesting and complex architectures, a second series of experiments were carried out to target a series of miktoarm block copolymers containing polylactide arms of different stereochemistry. In particular, we wished to assess the role of stereocomplexation of enantiomeric polylactides on the behavior or amphiphilic miktoarm block copolymers. The mechanical and thermal properties of polylactide strongly influence both their relative and absolute stereochemistry. As the isotactic polylactides, poly(L-lactide) (L-PLA or P(L)LA) and poly(D-lactide) (D-PLA or P(D)LA), are crystalline thermoplastics, atactic polylactide, poly(*rac*-lactide) (*rac*-PLA), derived from racemic mixture of D- and L-lactides is amorphous. Moreover, numerous reports on the distinctive morphology and mechanical properties as well as drug delivery applications of these stereocomplexes have appeared since Ikada reported the stereocomplex formation from mixtures of L-PLA and D-PLA.[29−31]

To generate miktoarm diblocks with symmetric lactide arms, the carbonate functional monomethyl ether PEG was ring-opened with aminopentanol in methylene chloride (0.1 M) to give a macroinitiator containing two primary alcohols capable of initiating the ROP of lactide. Purification was accomplished by polymer precipitation. From this macroinitiator, L-, D- or *rac*-lactide was polymerized in methylene chloride using a thiourea/sparteine catalyst mixture to give near quantitative conversion of monomer to polymer, generating Y-shaped polymers of PEG-P(L)PLA-P(L)LA, PEG-P(D)LA-P(D)LA, and PEG-*rac*PLA-*rac*PLA, respectively. The molecular weight of the carbonate-functional PEG macroinitiators increased to ~15000 g/mol for the Y-shaped copolymers and the polydispersities were narrow

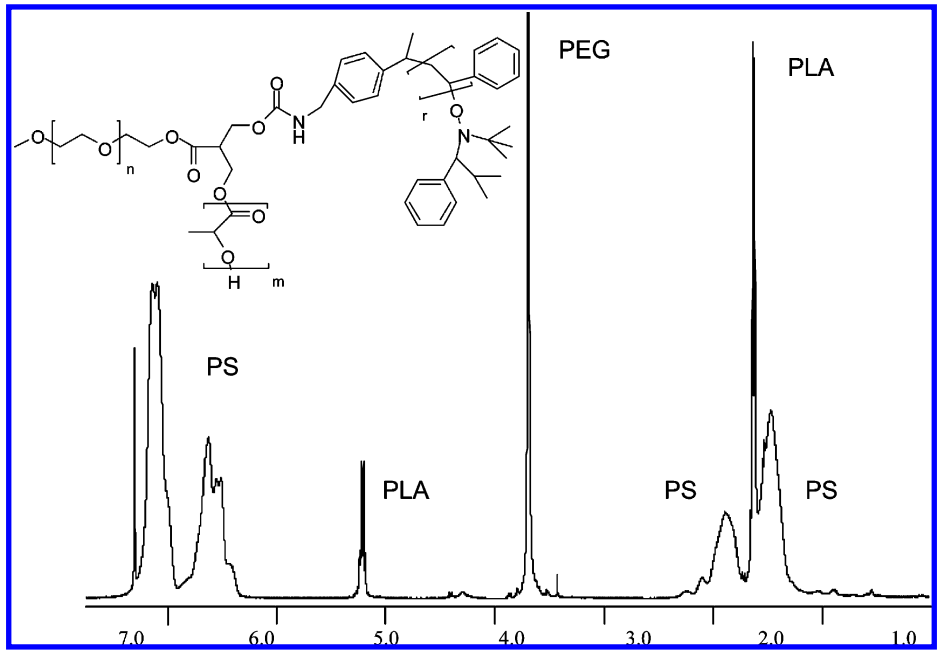

Figure 1. ^{1}H NMR ($CDCl_3$) of PEG-PS-PLA ABC miktoarm terpolymer.

(PDI < 1.10) with no evidence of homopolymer contamination (Table 1). As a control, a diblock copolymer prepared by the initiation of L-lactide (DP 35) from the monomethylether PEG was analyzed in the GPC together with the Y-shaped copolymer. As expected, the Y-shapes copolymer exhibited the higher molecular weight than the linear copolymer.

Alternatively, *tert*-butyldimethylsilyl protected aminopentanol was reacted with the carbonate functional monomethylether PEG, generating a primary alcohol and a protected alcohol on ring-opening. The ROP of L-lactide (target DP = 35) initiated from the primary alcohol of the macroinitiator was accomplished in methylene chloride in the presence of thiourea/sparteine. Upon quantitative monomer conversion, acetic anhydride was added to generate a methylester end-group. Interestingly, the catalyst used to facilitate polymerization also affected the capping of the end-group and ^{1}H NMR confirmed the structure as the quartet at ~4.35 ppm was completely removed. Isolation of this two-step, one-pot synthesis by precipitation produced a narrowly dispersed diblock copolymer with predictable molecular weight and end-group fidelity. Removal of the *tert*-butyldimethylsilyl protecting group using boron trifluoride diethyletherate generated an alcohol at the block junction that was used to initiate the second ROP of D-lactide with a targeted DP of 35 in methylene chloride using thiourea/sparteine, yielding a miktoarm stereoblock copolymer. GPC was used to demonstrate the successful chain extension between each transformation, Figure 2. Differential scanning calorimetry (DSC) of the resultant PEG-P(L)LA-P(D)LA miktoarm triblock copolymer revealed a higher melting point (T_m = 185 °C) than that observed for either the PEG-P(L)LA-P(L)LA or PEG-P(D)LA-P(D)LA (T_m = 145 °C, Figure 3), indicating that the miktoarm PEG-P(L)LA-P(D)LA forms stable stereocomplexes from the melt. In all thermograms the melting of PEG can also be observed at ~45 °C.

To study the role of architecture and stereocomplexation on the micellization behavior, we investigated a series of linear and Y-shaped block co/ter-polymers (Table 2). Here we anticipated that the stereocomplex itself might affect the core of resulting micelles, also observed by Leroux et al.,[31] thus lowering the critical micelle concentration. For this study the CMC, aggregation number (N_w), and size were studied for a

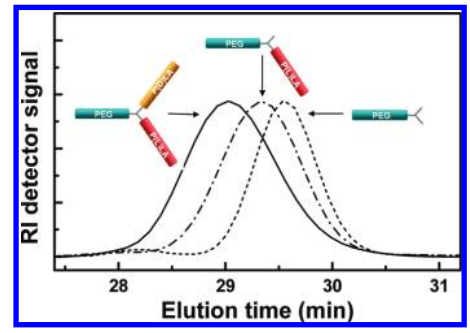

Figure 2. GPC curve for PEG (short dash), PEG-P(L)LA (dash dot), and PEG-P(L)LA-P(D)LA (solid).

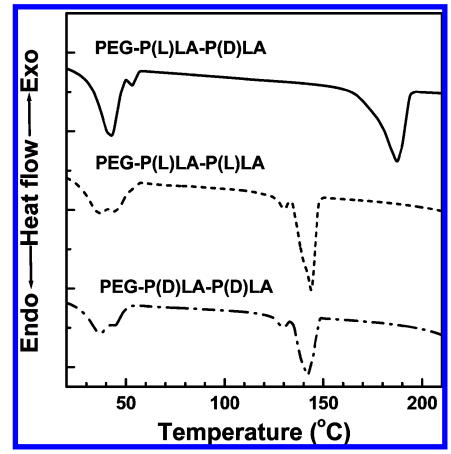

Figure 3. DSC thermogram of stereoblock PEG-P(L)LA-P(D)LA, stereoregular PEG-P(L)LA-P(L)LA and PEG-P(D)LA-P(D)LA miktoarm polymers.

selection of structures made and shown in Table 2. Linear PEG-P(L or D)LA block copolymers were also included as reference (Table 2, entries 1−3). In general, the CMC value is a strong evidence for self-assembly of an amphiphilic polymer into micellar structures but it is also an important parameter to anticipate the in vivo performance in the large volume of blood (5−6 L per 50−60 kg human body). Polymers with higher CMC values are usually less suitable as drug delivery vehicles because

Table 2. Properties of Linear and Y-Shaped PEG-PLA Micelles

	polymer[a]	CMC (mg/L)	N_w[b]	diameter (nm)	polydispersity[c]
linear	PEG-P(D)LA(5k-2k)	25.1	40	24.2	0.08
	PEG-P(L)LA(5k-2k)	24.0	43	23.8	0.07
	PEG-P(D)LA + PEG-P(L)LA	15.8	30	28.1	0.10
Y-shape	PEG-P(L)LA-P(D)LA (5k-2k-2k)	15.1	18	26.4	0.11
	PEG-P(D)LA-P(D)LA (5k-2k-2k)	20.0	27	29.3	0.09
	PEG(5k)-P(L)LA-P(L)LA (5k-2k-2k)	19.1	25	27.6	0.10
	PEG-P(D)LA-P(D)LA + PEG-P(L)LA-P(L)LA	10.0	20	32.3	0.13

[a] Parentheses after polymer denotes average molecular weight in (k)g/mol. [b] Aggregation number. [c] Size polydispersity values obtained from DLS measurements in which lower values indicate a more narrowly dispersed system.

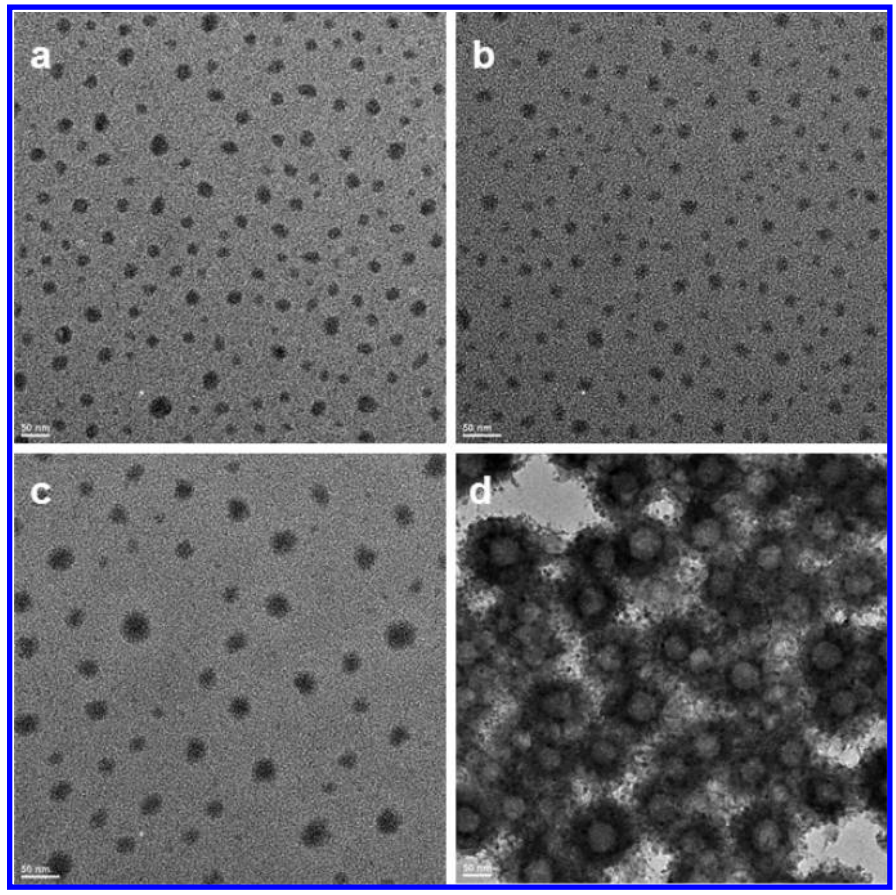

Figure 4. TEM images for micelles obtained from (a) diblock mixture of PEG-P(D)LA and PEG-P(L)LA, (b) Y-shaped PEG-P(L)LA-P(D)LA, (c) Y-shaped mixture of PEG-P(L)LA-P(L)LA and PEG-P(D)LA-P(D)LA, and (d) paclitaxel-loaded Y-shaped stereomixture.

they will easily dissociate after being administrated due to dilution by the blood.

Pyrene was used to determine the CMC by monitoring the ratio of intensities in the excitation spectra (from 334 to 337 nm, data not shown), which provides a measure of the partitioning of pyrene into the hydrophobic core.[32] At lower polymer concentrations, the intensity ratio of I_{337}/I_{334} changed slightly, but the intensity peak increased abruptly near the CMC. From Table 2 it is clear that stereocomplexation results in a reduced CMC value as compared to the corresponding linear or Y-shaped polymer due to the formation of a more stable core, that is, the linear stereocomplex composed of PEG-P(D)LA mixed with PEG-P(L)LA (entry 3) has a lower CMC than a single PEG-P(D)LA (entry 1) or PEG-P(L)LA (entry 2), respectively. Similarly, the Y-shaped stereoblock PEG-P(D)LA-P(L)LA (entry 4) has a lower CMC than a single PEG-P(D)LA-P(D)LA (entry 5) and PEG-P(L)LA-P(L)LA (entry 6). The lowest CMC (10 mg/mL) was found in the stereocomplex of PEG-P(L)LA-P(L)LA mixed with PEG-P(D)LA-P(D)LA (entry 7).

Furthermore, the aggregation number and hydrodynamic diameter are consistent with the formation of spherical micelles, which typically contains 16−60 unimers per micelle and with a hydrodynamic diameter of 20−60 nm.[33] The micelles for both the diblock and Y-shaped PEG-PLA, as shown in the TEM images in Figure 4, are spherical nanoparticles with a range of sizes from ~24 to 33 nm. The polydispersity values obtained from DLS measurements (Table 2) indicate that the micelles have a narrow size distribution. After the incorporation of paclitaxel, the corresponding paclitaxel-loaded micelles were bigger resulting from the enlargement of the core due to the drug content (Table 3). The polydispersities especially for paclitaxel-loaded stereocomplex micelles were still low after the encapsulation of paclitaxel as shown in Table 3 and Figure 4. These micelles with narrow size distribution are promising carriers for targeted drug delivery via the enhanced permeation and retention effect from the hyperpermeable angiogenic vasculature surrounding tumors.[34] In addition, they can yield a more desirable biodistribution when compared to micelles formed from conventional block copolymers with a wider size distribution. Paclitaxel-loaded stereocomplex micelles show a hollow nanostructure possibly due to the interaction between the stereocomplex and paclitaxel (Figure 4d). The stereocomplex

Table 3. Size and Size Distribution of Paclitaxel-Loaded Y-Shaped PEG-PLA Micelles

	paclitaxel-loaded micelles	
polymer[a]	diameter (nm)	polydispersity[b]
PEG-P(D)LA-P(D)LA (5k-2k-2k)	221.6	0.20
PEG-P(L)LA-P(D)LA (5k-2k-2k)	160.0	0.13
PEG-P(D)LA-P(D)LA + PEG-P(L)LA-P(L)LA	152.5	0.12

[a] Parentheses after polymer denotes average molecular weight in (k)g/mol. [b] Size polydispersity values obtained from DLS measurements in which lower values indicate a more narrowly dispersed system.

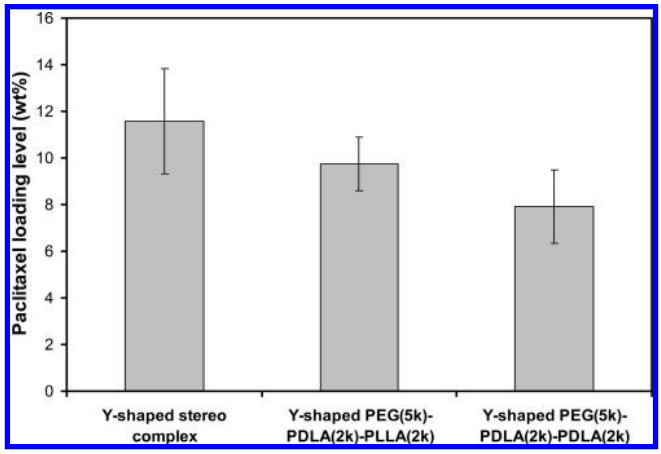

Figure 5. Paclitaxel loading content in Y-shaped stereocomplex mixture of PEG-P(D)LA-P(D)LA and PEG-P(L)LA-P(L)LA, Y-shaped stereoblock PEG-P(L)LA-P(D)LA, and Y-shaped stereoregular PEG-P(D)LA-P(D)LA (5k-2k-2k) micelles.

micelles without paclitaxel and paclitaxel-loaded Y-shaped PEG-P(D)LA-P(D)LA(5k-2k-2k) micelles, which were fabricated using the same protocol, do not show a vesicle structure (Figures S5 and S6). These unique features (i.e., narrow size distribution and hollow structure) may yield a constant paclitaxel release rate as paclitaxel molecules may travel a similar distance to diffuse toward the external aqueous environment.

Paclitaxel can be encapsulated into the core of the micelles by physical entrapment like hydrophobic interactions between drug and hydrophobic block of polymers. Drug loading during the dialysis process is affected by nature of the solvent, solvent exchange rate, dialysis medium used, and initial drug loading level.[35] Before the dialysis, sonication was carried out to reduce the particle size. In brief, 5 mg of block copolymer and paclitaxel (1 mg) were dissolved in 1 mL of acetone. The drug and polymer solution was added dropwise to DI water (10 mL) when being sonicated for 10 min. The solution was then dialyzed against 1000 mL of DI water for 48 h using a dialysis bag with molecular weight cutoff of 1000 Da. The water was changed every 2 h for the first 6 h and once again the next day. No paclitaxel precipitates were observed especially for Y-shaped stereocomplex samples and paclitaxel loading level was also increased with the sonication approach. For example, Y-shaped PEG-P(D)LA-P(D)LA micelles fabricated with and without sonication yielded paclitaxel loading of 7.9 and 5.0%, respectively. Furthermore, stereocomplexation resulted in a higher loading content of paclitaxel. As shown in Figure 5, the loading level of paclitaxel was 7.9 and 11.6 wt % for Y-shaped PEG-P(D)LA-P(D)LA micelles and Y-shaped PEG-P(D)LA-P(D)LA/PEG-P(L)LA-P(L)LA stereocomplex micelles, respectively. A similar phenomenon was also reported by Chen et al. for loading of rifampin (an antibiotic).[36]

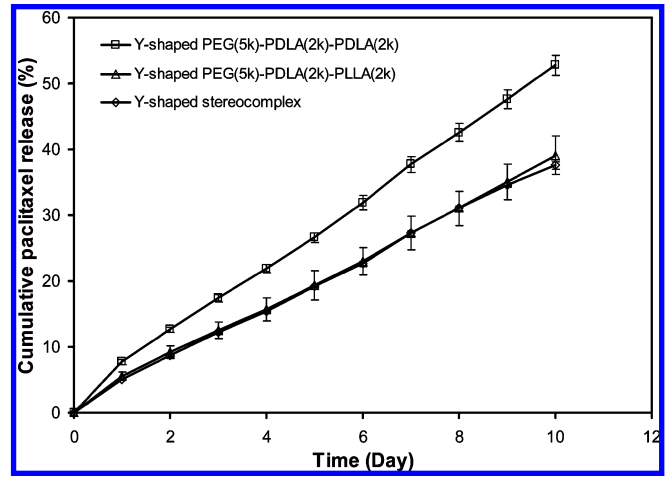

Figure 6. In vitro drug release profiles of paclitaxel from paclitaxel-loaded micelles incubated at 37 °C in PBS buffer (pH 7.4).

Figure 6 shows the cumulative release of paclitaxel from the micelles, incubated in PBS buffer (pH 7.4) at 37 °C (simulated physiological conditions). There was no significant initial burst release from all types of the micelles as only a maximum paclitaxel release of 8% was observed during the first 24 h. A sustained release and near zero-ordered release kinetics of paclitaxel was obtained from all types of micelles over the testing period of 10 days. This is most likely due to the narrow size distribution and molecular dispersion of paclitaxel molecules within the inner wall of the hollow micelles, resulting in a short and near constant path for the diffusion of dissolved paclitaxel molecules. The paclitaxel release was slower from Y-shaped PEG-P(D)LA-P(D)LA/PEG-P(L)LA-P(L)LA stereocomplex mixture as well as Y-shaped PEG-P(L)LA-P(D)LA stereoblock micelles than that from single Y-shaped PEG-P(D)LA-P(D)LA micelles. For example, the amount of paclitaxel released from Y-shaped PEG-P(D)LA-P(D)LA micelles after 10 days was more than 50%, whereas only 30% of the paclitaxel was released from Y-shaped stereocomplex micelles. This is likely caused by stronger interaction between the stereocomplexes and paclitaxel molecules.

Conclusion

In this report, we demonstrated the use of carbonate functionalized macro initiators as a key building block for novel molecular architectures. More precisely, different routes to ABC miktoarm terpolymers were shown using functional amines directed to a PEG backbone via a carbamate link. Both NMP and ROP were used, individually or in combination, to add the additional two arms. Resulting PEG-P(L)LA-P(D)LA miktoarm terpolymers formed stereocomplexes in bulk and were also shown to form stabilized micelles in an aqueous solution. Our generic approach is both simple and versatile and provides a useful synthetic platform in the design of macromolecular architectures for various biomedical applications. For proof of concept, this approach has been employed to synthesize Y-shaped PEG-P(L)LA-P(D)LA, PEG-P(D)LA-P(D)LA, and PEG-P(L)LA-P(L)LA polymers, which can form stereocomplex micelles with narrow size distribution. These micelles have demonstrated high capacity of paclitaxel loading and near zero-ordered paclitaxel release without significant initial burst.

Acknowledgment. F.N. thanks the Swedish Research Council (VR) for financial support. Further support comes from the NSF Center on Polymer Interfaces and Macromolecular Assemblies

(CPIMA: NSF-DMR 0213618) and a NSF-GOALI grant (NSF-CHE-0645891). J.P.K.T. and Y.Y.Y. thank the Institute of Bioengineering and Nanotechnology, Agency for Science, Technology and Research, Singapore, for financial support. We thank Teddie Magbitang and Dolores Miller for analytical support.

Supporting Information Available. We provide additional results on GPC, light scattering, and TEM characterizations. This material is available free of charge via the Internet at http://pubs.acs.org.

References and Notes

(1) (a) Kamber, N. E.; Jeong, W.; Waymouth, R. M.; Pratt, R. C.; Lohmeijer, B. G. G.; Hedrick, J. L. *Chem. Rev.* **2007**, *107*, 5813–5840. (b) Hawker, C. J.; Wooley, K. L. *Science* **2005**, *309*, 1200–1205. (c) Kolb, H. C.; Finn, M. G.; Sharpless, K. B. *Angew. Chem., Int. Ed.* **2001**, *40*, 2004–2021.

(2) (a) Choi, J.; Hermans, T. M.; Lohmeijer, B. G. G.; Pratt, R. C.; Dubois, G.; Frommer, J.; Waymouth, R. M.; Hedrick, J. L. *Nano Lett.* **2006**, *6*, 1761–1764. (b) Freer, E. M.; Krupp, L. E.; Hinsberg, W. D.; Rice, P. M.; Hedrick, J. L.; Cha, J. N.; Miller, R. D.; Kim, H.-C. *Nano Lett.* **2005**, *5*, 2014–2018. (c) Magbitang, T.; Lee, V. Y.; Cha, J. N.; Wang, H.-L.; Chung, R.; Miller, R. D.; Dubois, G.; Volksen, W.; Kim, H.-C.; Hedrick, J. L. *Angew. Chem., Int. Ed.* **2005**, *44*, 7574–7580.

(3) Frechet, J. M. J.; Tomalia, D. A. *Dendrimers and Other Dendritic Polymers*; Wiley: New York, 2001; ISBN 0471638501.

(4) (a) Percec, V.; Ahn, C.-H.; Ungar, G.; Yeardley, D. J. P.; Möller, M.; Sheiko, S. S. *Nature* **1998**, *391*, 161–164. (b) Stupp, S. I.; LeBonheur, V.; Walker, K.; Li, L. S.; Huggins, K. E.; Keser, M.; Amstutz, A. *Science* **1997**, *276*, 384–389. (c) Hermans, T. M.; Choi, J.; Lohmeijer, B. G. G.; Dubois, G.; Pratt, R. C.; Kim, H.-C.; Waymouth, R. M.; Hedrick, J. L. *Angew. Chem., Int. Ed.* **2006**, *45*, 6648–6652.

(5) (a) Trollsas, M.; Atthoff, B.; Claesson, H.; Hedrick, J. L. *Macromolecules* **1998**, *31*, 3439–3445. (b) Hedrick, J. L.; Trollsas, M.; Hawker, C. J.; Atthoff, B.; Claesson, H.; Heise, A.; Miller, R. D.; Mecerreyes, D.; Jerome, R.; Dubois, Ph. *Macromolecules* **1998**, *31*, 8691–8705. (c) Heise, A.; Nguyen, C.; Malek, R.; Hedrick, J. L.; Frank, C. W.; Miller, R. D. *Macromolecules* **2000**, *33*, 2346–2354.

(6) Mansky, P.; Liu, Y.; Huang, E.; Russell, T. P.; Hawker, C. *Science* **1997**, *275*, 1458–1460.

(7) Cho, B.-K.; Jain, A.; Mahajan, S.; Ow, H.; Gruner, S. M.; Wiesner, U. *J. Am. Chem. Soc.* **2004**, *126*, 4070–4071.

(8) Chen, Z.; Cui, H.; Hales, K.; Li, Z.; Qi, K.; Pochan, D. J.; Wooley, K. L. *J. Am. Chem. Soc.* **2005**, *127*, 8592–8593.

(9) Connor, E. F.; Nyce, G. W.; Myers, M.; Mock, A.; Hedrick, J. L. *J. Am. Chem. Soc.* **2002**, *124*, 914–915.

(10) (a) Dove, A. P.; Pratt, R. C.; Lohmeijer, B. G. G.; Waymouth, R. M.; Hedrick, J. L. *J. Am. Chem. Soc.* **2005**, *127*, 13798–13799. (b) Pratt, R. C.; Lohmeijer, B. G. G.; Long, D. A.; Lundberg, P. N. P.; Dove, A. P.; Li, H.; Wade, C. G.; Waymouth, R. M.; Hedrick, J. L. *Macromolecules* **2006**, *39*, 7863–7871.

(11) Pratt, R. C.; Lohmeijer, B. G. G.; Long, D. A.; Waymouth, R. M.; Hedrick, J. L. *J. Am. Chem. Soc.* **2006**, *128*, 4556–4557.

(12) Zhang, L.; Nederberg, F.; Messman, J. M.; Pratt, R. C.; Hedrick, J. L.; Wade, C. G. *J. Am. Chem. Soc.* **2007**, *129*, 12610–12611.

(13) Coulembier, O.; Kiesewetter, M. K.; Mason, A.; Dubois, P.; Hedrick, J. L.; Waymouth, R. M. *Angew. Chem., Int. Ed.* **2007**, *46*, 4719–4721.

(14) (a) Culkin, D. A.; Jeong, W.; Csihony, S.; Gomez, E. D.; Balsara, N. P.; Hedrick, J. L.; Waymouth, R. M. *Angew. Chem., Int. Ed.* **2007**, *46*, 2627–2630. (b) Jeong, W.; Hedrick, J. L.; Waymouth, R. M. *J. Am. Chem. Soc.* **2007**, *129*, 8414–8415.

(15) (a) Pratt, R. C.; Nederberg, F.; Waymouth, R. M.; Hedrick, J. L. *Chem. Commun.* **2008**, 114–116. (b) Nederberg, F.; Trang, V.; Pratt, R. C.; Mason, A. F.; Frank, C. W.; Waymouth, R. M.; Hedrick, J. L. *Biomacromolecules* **2007**, *8*, 3294–3297.

(16) Goodwin, A. P.; Lam, S. S.; Frechet, J. M. J. *J. Am. Chem. Soc.* **2007**, *129*, 6994–6995.

(17) Ochiai, B.; Satoh, Y.; Endo, T. *Green Chem.* **2005**, *7*, 765–767.

(18) (a) Lopes, N. M.; Adams, E. G.; Pitts, T. W.; Bhuyan, B. K. *Cancer Chemother. Pharmacol.* **1993**, *32*, 235–242. (b) Wani, M. C.; Taylor, H. L.; Wall, M. E.; Coggon, P.; McPhail, A. T. *J. Am. Chem. Soc.* **1971**, *93*, 2325–2327.

(19) Weiss, R. B.; Donehower, R. C.; Wiernik, P. H.; Ohnuma, T.; Gralla, R. J.; Trump, D. L.; Baker, J. R.; Vanecho, D. A.; Vonhoff, D. D.; Leyland-Jones, B. *J. Clin. Oncol.* **1990**, *8*, 1263–1268.

(20) Liggins, R. T.; D'Amours, S.; Demetrick, J. S.; Machan, L. S.; Burt, H. M. *Biomaterials* **2000**, *21*, 1959–1969.

(21) (a) Westedt, U.; Kalinowski, M.; Wittmar, M.; Merdan, T.; Unger, F.; Fuchs, J.; Schäller, S.; Bakowsky, U.; Kissel, T. *J. Controlled Release* **2007**, *119*, 41–51. (b) Potineni, A.; Lynn, D. M.; Langer, R.; Amiji, M. M. *J. Controlled Release* **2003**, *86*, 223.

(22) (a) Cheng, C.; Wei, H.; Shi, B.-X.; Cheng, H.; Li, C.; Gu, Z.-W.; Cheng, S.-X.; Zhang, X.-Z.; Zhuo, R.-X. *Biomaterial* **2008**, *29*, 497–505. (b) Hamaguchi, T.; Matsumura, Y.; Suzuki, M.; Shimizu, K.; Goda, R.; Nakamura, I.; Nakatomi, I.; Yokoyama, M.; Kataoka, K.; Kakizoe, T.; British, J. *Cancer* **2005**, *92*, 1240–1246. (c) Liu, S. Q.; Tong, Y. W.; Yang, Y.-Y. *Biomaterial* **2005**, *26*, 5064–5074.

(23) (a) Xie, J.; Wang, C.-H. *Pharm. Res.* **2005**, *22*, 2079–2090. (b) Liu, Y.; Chen, G.-S.; Chen, Y.; Cao, D.-X.; Ge, Z.-Q.; Yuan, Y.-J. *Bioorg. Med. Chem.* **2004**, *12*, 5767–5775.

(24) Tan, J. P. K.; Kim, S. H.; Nederberg, F.; Appel, E. A.; Waymouth, R. M.; Zhang, Y.; Hedrick, J. L.; Yang, Y. Y. *Small* **2009**, accepted for publication.

(25) Seow, W. Y.; Xue, J. M.; Yang, Y.-Y. *Biomaterials* **2007**, *28*, 1730–1740.

(26) (a) Hadjichristidis, N.; Iatrou, H.; Behal, S. K.; Chludzinski, J. J.; Disko, M. M.; Garner, R. T.; Liang, K. S.; Lohse, D. J.; Milner, S. T. *Macromolecules* **1993**, *26*, 5812–5815. (b) He, T.; Li, D.; Sheng, X.; Zhao, B. *Macromolecules* **2004**, *37*, 3128–3135. (c) Gao, H.; Matyjaszewski, K. *Macromolecules* **2006**, *39*, 7216–7223. (d) Li, Z.; Kesselman, E.; Talmon, Y.; Hillmyer, M. A.; Lodge, T. P. *Science* **2004**, *306*, 98–101. (e) Rieger, J.; Coulembier, O.; Dubois, P.; Bernaerts, K. V.; Du Prez, F. E.; Jerome, R.; Jerome, C. *Macromolecules* **2005**, *38*, 10650–10657.

(27) (a) Bosman, A. W.; Vestberg, R.; Heumann, A.; Frechet, J. M. J.; Hawker, C. J. *J. Am. Chem. Soc.* **2003**, *125*, 715–728. (b) Hawker, C. J.; Bosman, A. W.; Harth, E. *Chem. Rev.* **2001**, *101*, 3661–3688.

(28) Depending on the manufacturer of the monomethylether PEG starting material, a double molecular weight peak might accompany the main GPC peak, which may translate into a weak high end shoulder of the final structure; see Supporting Information.

(29) Ikada, Y.; Jamshidi, K.; Tsuji, H.; Hyon, S. H. *Macromolecules* **1987**, *20*, 904–906.

(30) Chung, H. J.; Lee, Y.; Park, T. G. *J. Controlled Release* **2008**, *127*, 22–30.

(31) Kang, N.; Perron, M.-E.; Prudhomme, R. E.; Zhang, Y.; Gaucher, G.; Leroux, J.-C. *Nano Lett.* **2005**, *5*, 315–319.

(32) (a) Wilhelm, M.; Zhao, C.-L.; Wang, Y.; Xu, R.; Winnik, M. A.; Mura, J.-L.; Riess, G.; Croucher, M. D. *Macromolecules* **1991**, *24*, 1033–1040. (b) Astafieva, I.; Zhong, X. F.; Eisenberg, A. *Macromolecules* **1993**, *26*, 7339–7352. (c) Jones, M.-C.; Leroux, J.-C. *Eur. J. Pharm. Biopharm.* **1999**, *48*, 101–111.

(33) Booth, C.; Attwood, D. *Macromol. Rapid Commun.* **2000**, *21*, 501–527.

(34) Matsumura, Y.; Maeda, H. *Cancer Res.* **1986**, *46*, 6387–6392.

(35) (a) Chaw, C. S.; Chooi, K. W.; Liu, X. M.; Tan, C. W.; Wang, L.; Yang, Y.-Y. *Biomaterials* **2004**, *25*, 4297–4308. (b) Kwon, G.; Naito, M.; Yokoyama, M.; Okano, T.; Sakurai, Y.; Kataoka, K. *J. Controlled Release* **1997**, *48*, 195–201.

(36) Chen, L.; Xie, Z.; Hu, J.; Chen, X.; Jing, X. *J. Nanopart. Res.* **2007**, *9*, 777–785.

BM900056G